arXiv:1303.6965v1 [cond-mat.mes-hall] 27 Mar 2013

Full Counting Statistics of Photons Emitted by Double Quantum Dot

Canran Xu and Maxim G. Vavilov
Department of Physics, University of Wisconsin-Madison, Wisconsin 53706, USA

(Dated: March 27, 2013)

We analyze the full counting statistics of photons emitted by a double quantum dot (DQD) to a high-quality microwave transmission line due to the dipole coupling. We show that at the resonant condition between the energy splitting of the DQD and the photon energy in the transmission line, photon statistics exhibits both a sub-Poissonian distribution and antibunching. In the ideal case, when the system decoherence stems only from photodetection, the photon noise is reduced below one-half of the noise for the Poisson distribution. The photon distribution remains sub-Poissonian even at moderate decoherence in the DQD.

PACS numbers: 73.23.-b, 73.63.Kv, 42.50.Ar

Introduction. The statistics of photons emitted by an electric current depends on an electron state of a conductor. If electric current were classical, photon field would be in a coherent state[1] with the Poisson noise. A quantum electron system with strong inelastic processes is characterized by the thermal distribution and produce black-body radiation with super-Poissonian statistics of emitted photons. However, if the electron distribution is far from equilibrium, the photon counting statistics may become sub-Poissonian.[2,3]

Several experimental approaches have recently been developed to study statistics of photons in the GHz frequency range. Experiments[4,5] measure the photon statistics in a steady state of high quality resonator and distinguish between the thermal source and a coherent drive. Photon noise of a quantum point contact at finite bias was also investigated using the amplifier technique.[6] An alternative approach to study photon statistics utilizes photon counter.[8] An individual photon counter can provide information about statistics of emitted photons, while a system with two counters can be used to measure the second order intensity correlation function $g^{(2)}_{\rm ph}(\tau)$, see *e.g.* Ref. 7, which represents the correlations in observing two photons at two moments separated by time τ.

In this paper we analyze the statistics of photon radiation from a double quantum dot coupled to a high-quality microwave transmission line, a system that was recently experimentally studied by several groups.[9–11] In the absence of decoherence processes in the DQD, the transition from its excited state with energy E_e to the ground state with energy E_g occur only via emission of a photon to the transmission line. In this case, dependences of the current and the average photon number on energy difference $E_e - E_g$ exhibit resonant peaks at photon energy $\hbar\omega_0 = E_e - E_g$. At the same condition, we find the suppression of noise in charge transfer and photon emission, indicating on sub-Poisson statistics.

We also evaluate the second order correlation function $g^{(2)}_{\rm ph}(\tau)$. We find that this function is reduced for time intervals shorter than the typical time of an electron passage through a DQD, thus reflecting an electronic origin of photon emission in the resonator. We also calculate the distribution function for photon counting, which differs significantly from the Poisson distribution. Finally, we analyze the effect of energy and phase relaxation of electron states in the DQD. We find that while pure dephasing has a weak influence on the photon statistics, inelastic energy relaxation changes photon counting statistics towards super-Poissonian.

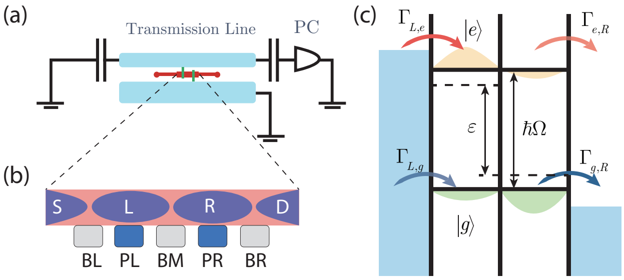

FIG. 1. (Color online) (a) An illustration of a DQD and a transmission line coupled to a photon counter (PC). (b) In the DQD, electrons are confined to the left (L) and right (R) dots by barrier gates BL, BM, and BR that also control electron tunneling rates between the source, S, and the left dot, the left and right dots, and the right dot and the drain, D, respectively. Electrostatic energies of two quantum dots are defined by the plunger gates, PL and PR, and the PL gate is also connected to an antinode of the transmutation line. (c) Electronic states of the DQD are presented in both the eigenstate basis (solid lines) and the left–right basis (dashed lines). Tunneling from the left lead to the ground/excited state with rate $\Gamma_{L,g/e}$, and from the ground/excited state to the right lead with rate $\Gamma_{g/e,R}$ are illustrated by arrows.

Model. We study statistical properties of charge transfer through the DQD and photon emission to the transmission line. The Hamiltonian for a system of coupled DQD and the transmission line, shown in Fig. 1, is presented as a combination of three terms, $H = H_{\rm DQD} + H_{\rm ph} + H_{\rm int}$. The non-interacting DQD near a triple point in its electrostatic stability diagram[12] is represented by

$$H_{\rm DQD} = \frac{1}{2}\hbar\varepsilon\tau_z + \hbar\mathcal{T}\tau_x, \tag{1}$$

in the basis of electron states in the left, $|L\rangle$, and right, $|R\rangle$, quantum dots with electrostatic level bias

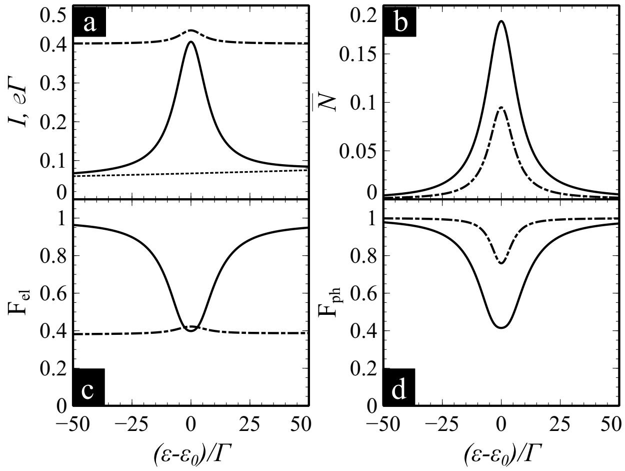

FIG. 2. (Color online) Dependences of (a) the electric current I through the DQD, (b) the average photon number $\bar{N}$ in the transmission line, (c) the electron Fano factor F_{el} and (d) the Fano factor F_{ph} for emitted photons are shown as functions of the electrostatic bias $\hbar\varepsilon$ near the resonance at $\hbar\varepsilon_0$ with $\varepsilon_0 = \sqrt{\omega_c^2 - 4\mathcal{T}^2}$. Solid (dashed) lines represent the case for $\gamma_r = 0$ ($\gamma_r = 2\Gamma$). Other system parameters are $\Gamma_{l,r} = \Gamma$, $\omega_0 = 800\Gamma$, $\mathcal{T} = 200\Gamma$, $g_0 = 5\Gamma$, $\kappa = 2\Gamma$ and $\gamma_\phi = 0$. Dotted line in panel (a) refers to elastic electric current through a non-interacting DQD.

ε and the tunneling amplitude $\mathcal{T}$; in this basis, $\tau_z = |R\rangle\langle R| - |L\rangle\langle L|$ and $\tau_x = |R\rangle\langle L| + |L\rangle\langle R|$. The term $H_{\text{ph}} = \hbar\omega_0 a^\dagger a$ represents a noninteracting photon mode in the transmission line. The interaction between charge and photon degrees of freedom is described by the Jaynes-Cummings Hamiltonian $H_{\text{int}} = \hbar g_0 \left(a^\dagger\sigma^- + a\sigma^+\right)$[13–16].

In further calculations, we use the eigenstates of the DQD Hamiltonian, Eq.(1), namely the ground, $|g\rangle$, and excited, $|e\rangle$, states:

$$
\begin{aligned}
|e\rangle &= \cos(\theta/2)\,|L\rangle + \sin(\theta/2)\,|R\rangle\,, \\
|g\rangle &= -\sin(\theta/2)\,|L\rangle + \cos(\theta/2)\,|R\rangle\,.
\end{aligned} \tag{2}
$$

Here $\theta = \arctan(2\mathcal{T}/\varepsilon)$ characterizes the hybridization between states $|L\rangle$ and $|R\rangle$. The energy splitting between the eigenstates $\hbar\Omega = \hbar\sqrt{\varepsilon^2 + 4\mathcal{T}^2}$ can be tuned via gate voltages.[12] In the eigenstate basis, Eq. (2), the full Hamiltonian is reduced to

$$H = \frac{\hbar\Omega}{2}\sigma_z + \hbar\omega_0 a^\dagger a + \hbar g(a^\dagger\sigma^- + a\sigma^+), \tag{3}$$

where $g = g_0 \sin\theta$ is the effective electron–photon coupling constant, and the matrices $\sigma^- = |g\rangle\langle e|$, $\sigma^+ = |e\rangle\langle g|$ and $\sigma_z = |e\rangle\langle e| - |g\rangle\langle g|$ are defined in the eigenstate basis.

We analyze the behavior of the system with Hamiltonian Eq. (3) in the presence of decoherence in electron and photon degrees of freedom and tunneling of electrons between the DQD and the leads by employing the Born-Markov master equation for the full density matrix

$$\dot{\rho} = \mathcal{L}\rho = -\frac{i}{\hbar}\left[H, \rho\right] + \mathcal{D}_{\text{tot}}\rho. \tag{4}$$

Here, the first term on the r.h.s. of Eq. (4) describes the unitary evolution of the system and the second term accounts for the decoherence and tunneling processes in the DQD and the transmission line:

$$
\begin{aligned}
\mathcal{D}_{\text{tot}}\rho =& \kappa\mathcal{D}(a)\rho + \gamma_r\mathcal{D}(\sigma^-)\rho + \frac{\gamma_\phi}{2}\mathcal{D}(\sigma_z)\rho \\
&+ \Gamma_l\mathcal{D}(c_l^\dagger)\rho + \Gamma_r\mathcal{D}(c_r)\rho,
\end{aligned} \tag{5}
$$

where $\mathcal{D}(x)\rho = \left(2x\rho x^\dagger - x^\dagger x\rho - \rho x^\dagger x\right)/2$ is the Lindblad superoperator. Detection of a photon in the transmission line by a photodetector with rate κ is represented by the first term, $\kappa\mathcal{D}(a)\rho$ and the electron relaxation from the excited state $|e\rangle$ to the ground state $|g\rangle$ with rate γ_r is represented by $\gamma_r\mathcal{D}(\sigma^-)\rho$. Similarly the third term describes the dephasing of the DQD with rate γ_ϕ.

The last two terms in Eq. (5) account for the processes of loading state $|L\rangle$ from the source with tunneling rate Γ_l and unloading state $|R\rangle$ to the drain with tunneling rate Γ_r, see FIG. 1. The tunneling superoperators are expressed in terms of $c_r = |0\rangle\langle R|$ and $c_l^\dagger = |L\rangle\langle 0|$.[14]

For this model, one can evaluate both charge transfer and photon emission statistics. The charge transfer statistics has been discussed in the literature for similar systems[15,17–21] and we present main relations for charge transfer statistics through a DQD in the Supplementary Materials. Below we provide equations for photon statistics. We assume that photon detection is performed by an ideal detector so that all emitted photons are eventually captured by the detector. The latter assumption is justified for high quality superconducting transmission line which can be made practically lossless.

The probability distribution $P_n(t_0)$ to count n photons during measurement time t_0 is related to the generating function (GF) $\mathcal{G}(t_0, s)$ through a discrete Fourier transform with respect to counting field $\chi \in [0, 2\pi]$:

$$P_n(t_0) = \int_0^{2\pi} \mathcal{G}(t_0, e^{-i\chi})e^{i\chi n}\frac{d\chi}{2\pi}. \tag{6}$$

The GF $\mathcal{G}(t, s) = \text{Tr}\{\tilde{\rho}(t, s)\}$ is expressed in terms of the generalized density matrix $\tilde{\rho}(t, s) = e^{\mathcal{M}(s)t}\rho_{\text{st}}$, which is the solution of the master equation with parametric dependence on the counting field $s = e^{-i\chi}$:

$$\frac{d\tilde{\rho}(t, s)}{dt} = \mathcal{M}(s)\tilde{\rho}(t, s), \quad \mathcal{M}(s) = \mathcal{L} + (s-1)\mathcal{J}(a). \tag{7}$$

Here $\mathcal{J}(a)\rho = \kappa a\rho a^\dagger$ is the jump operator that describes the photon detection with transition rate κ and ρ_{st} is the steady state of the density matrix defined by Eq. (4) with $\mathcal{L}\rho_{\text{st}} = 0$.

To quantify the width of the distribution $P_n(t_0)$, we evaluate the photon noise Fano factor

$$F_{\text{ph}} = \frac{\langle n^2\rangle - \langle n\rangle^2}{\langle n\rangle}. \tag{8}$$

The Fano factor equals 1 for Poissonian processes, while for sub-(super-) Poissonian processes, the Fano factor is below(above) 1.[2]

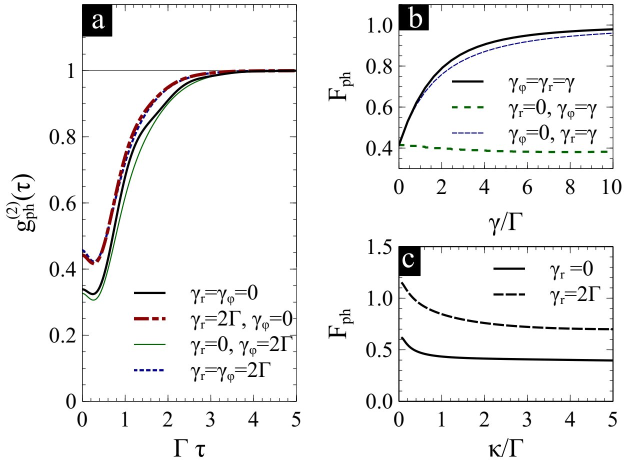

FIG. 3. (Color online) (a) The second order correlation function $g_{\rm ph}^2(2)(\tau)$ for photons as a function of time τ at resonant condition $\Omega = \omega_0$ for different values of energy, γ_r, and phase, γ_ϕ, relaxation rates. (b) The photon Fano factor $F_{\rm ph}$ as a function of relaxation rate γ in three cases $\gamma_r = \gamma_\phi = \gamma$ (solid line), $\gamma_r = \gamma$ and $\gamma_\phi = 0$ (dotted line), $\gamma_\phi = \gamma$ and $\gamma_r = 0$ (dashed line). (c) $F_{\rm ph}$ as a function of photon detection rate κ shows a flat behavior for $\kappa \gtrsim \Gamma$. Other system parameters in both panels are $\Gamma_{l,r} = \Gamma$, $\omega_0 = 800\Gamma$, $\mathcal{T} = 200\Gamma$, $g_0 = 5\Gamma$, $\kappa = 2\Gamma$ and $\gamma_\phi = 0$[for (a) and (b)].

For a lossless transmission line, the average photon count $\langle n\rangle = \kappa \bar{N} t_0$ during time t_0 is determined by the photon number $\bar{N} = \langle a^\dagger a\rangle_{\rm st} = {\rm Tr}\{\rho_{\rm st} a^\dagger a\}$ in the transmission line and the photon detection rate κ.[22] If the measurement time exceeds the characteristic system memory time, the Fano factor is t_0-independent and can be evaluated as a time integral:[23,24]

$$F_{\rm ph} = 1 + 2\kappa\bar{N}\int_0^\infty \left(g^{(2)}_{\rm ph}(\tau) - 1\right) d\tau. \tag{9}$$

Here, the second order correlation function $g^{(2)}_{\rm ph}(\tau)$ is given by[7]

$$g^{(2)}_{\rm ph}(\tau) = \frac{\langle a^\dagger a^\dagger(\tau) a(\tau) a\rangle}{\langle a^\dagger a\rangle^2} = \frac{{\rm Tr}\left\{a^\dagger a e^{\mathcal{L}\tau}\left(a\rho_{\rm st} a^\dagger\right)\right\}}{{\rm Tr}\left\{a^\dagger a\rho_{\rm st}\right\}^2}. \tag{10}$$

This function characterizes the joint probability to observe two photons separated by time interval τ and its asymptotic value is 1 at long times. In particular, photon antibunching (bunching) occurs when $g^{(2)}_{\rm ph}(0)$ is smaller (greater) than 1.

We discuss alternative methods of calculating statistical properties of photon emission in Sec. S.I. of the Supplementary Materials. We note that one can also apply similar formalism to evaluate cross-correlation functions of electron charge transfer and photon emission, which will be discussed elsewhere. Experimental observation of such cross–correlations is a challenging task, but can be achieved by combining charge sensing measurements[25] and photon detection.[8]

Results. Below we consider a DQD with equal tunneling rates through left and right contacts, $\Gamma_{l,r} = \Gamma$, and the interdot tunneling amplitude $\mathcal{T} = 200\Gamma$. We take $\omega_0 = 800\Gamma$, the photon relaxation rate $\kappa = 2\Gamma$ and the electron-photon bare coupling $g_0 = 5\Gamma$.

In FIG. 2 we present dependence of (a) electric current I, (b) the average number of photons in the transmission line, $\bar{N} = \langle a^\dagger a\rangle_{\rm st}$, (c) the Fano factor of charge current, $F_{\rm el}$, and (d) the Fano factor for photon flux, $F_{\rm ph}$, Eq.(8). Solid lines in FIG. 2 are evaluated for an ideal quantum dot when the inelastic relaxation from excited to the ground state is absent. In this case, the amplitudes of electric current and the photon flux have a well pronounced peak at the resonant condition $\Omega = \omega_0$, while away from the resonance, photon production is suppressed, $\bar{N} \to 0$, and the current approaches $I_0 = e\mathcal{T}^2\Gamma/(\varepsilon^2 + 3\mathcal{T}^2)$ for elastic electron transfer through a non-interacting DQD,[26] shown by a dotted line in FIG. 2a. Fano factors for both electric current and photon flux are reduced below 1/2, indicating sub-Poissonian statsitics with strong suppression of charge and photon noise at the resonance.

Moderate inelastic relaxation changes the above picture. Because inelastic relaxation facilitates electron transfer through the DQD, the electric current exceeds I_0 even away from the resonance, $|\Omega - \omega_0| \gg \Gamma$, and only a weak enhancement of the current occurs at $\Omega = \omega_0$. The electron Fano factor is reduced below unity in the presence of energy relaxation and the resonant electron transfer with photon emission does not significantly affects $F_{\rm el}$. We still observe a resonant emission of photons, see dashed line in FIG. 2b, but the statistics of emitted photons is closer to Poissonian.

We study the properties of the second order correlation function $g^{(2)}_{\rm ph}(\tau)$, see FIG. 3a. The thick solid line shows $g^{(2)}_{\rm ph}(\tau)$ for an ideal DQD without inelastic relaxation and dephasing, $\gamma_{\rm r} = \gamma_\phi = 0$. Probability to observe two photons simultaneously is reduced, $g^{(2)}_{\rm ph}(0) < 1$, indicating photon antibunching. As τ becomes longer than the typical electron transfer time through the DQD, $\sim 1/\Gamma$, function $g^{(2)}_{\rm ph}(\tau)$ increases and eventually approaches its asymptote, $g^{(2)}_{\rm ph}(\tau \to \infty) = 1$. The integral in Eq. (9) with such $g^{(2)}_{\rm ph}(\tau)$ is negative and the photon noise Fano factor $F_{\rm ph} < 1$.

In the presence of inelastic relaxation in the DQD, $g^{(2)}_{\rm ph}(0)$ increases and $g^{(2)}_{\rm ph}(\tau)$ reaches its long-time asymptotic value 1 at shorter time scale. This behavior of $g^{(2)}_{\rm ph}(\tau)$ results in larger value of $F_{\rm ph}$. Pure dephasing, γ_ϕ, only smoothens $g^{(2)}_{\rm ph}(\tau)$, and has little effect on the integral in Eq. (9) and, consequently, on $F_{\rm ph}$.

To investigate dependence of $F_{\rm ph}$ on inelastic, γ_r, and dephasing, γ_ϕ, rates, we plot $F_{\rm ph}(\gamma_r, \gamma_\phi)$ as a function of γ_r and γ_ϕ in FIG. 3b. Pure dephasing, $\gamma_\phi = \gamma$ and $\gamma_r = 0$, has extremely weak effect on $F_{\rm ph}$ even for large values of γ_ϕ, while the inelastic relaxation, $\gamma_r = \gamma$ and $\gamma_\phi = 0$, quickly recovers $F_{\rm ph}$ to its Poissonian value, $F_{\rm ph} = 1$.

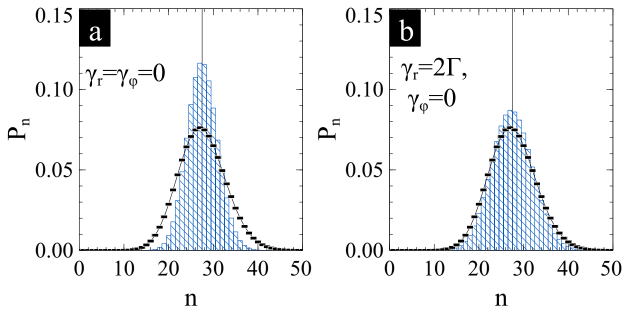

FIG. 4. (Color online) Probabilities P_n to have n emitted photons during time t_0 at resonance $\Omega = \omega_0$ for (a) an ideal DQD without decoherence of electronic states, $\gamma_r = \gamma_\phi = 0$ and $t_0 = 75/\Gamma$; (b) a DQD with inelastic relaxation $\gamma_r = 2\Gamma$, $\gamma_\phi = 0$ and $t_0 = 145/\Gamma$. Other system parameters in both panels are $\Gamma_{l,r} = \Gamma$, $\omega_0 = 800\Gamma$, $\mathcal{T} = 200\Gamma$, $g_0 = 5\Gamma$ and $\kappa = 2\Gamma$. A thin curve in both panels represents the corresponding Poisson distribution $P_n^{(P)} = e^{-\bar{n}}\bar{n}^n/n!$ with $\bar{n} = \sum_n nP_n$ equal to the average number of emitted photons.

Again, additional pure dephasing, $\gamma_\phi = \gamma_r = \gamma$, makes no significant corrections to $F_{\rm ph}$. The weak dependence of $F_{\rm ph}(\gamma_r, \gamma_\phi)$ on γ_ϕ is consistent with weak dependence of $g^{(2)}_{\rm ph}(\tau)$ on γ_ϕ, as discussed above.

We note that another Fano factor can be introduced to characterize the variance of the photon number $N = a^\dagger a$ in the steady state, $F^{(\rm st)}_{\rm ph} = (\langle N^2\rangle_{\rm st} - \langle N\rangle^2_{\rm st})/\langle N\rangle_{\rm st}$.[14] The quantity $F^{(\rm st)}_{\rm ph} = 1 + \langle N\rangle_{\rm st}(g^{(2)}_{\rm ph}(0) - 1)$ is given by instantaneous value $g^{(2)}_{\rm ph}(\tau = 0)$ in a steady state and does not represent time evolution of the photon field. Therefore, $F^{(\rm st)}_{\rm ph} < 1$ is an indicator of the photon antibunching. On the other hand, photon antibunching or bunching does not imply that the full counting statistics is sub- or super-Poissonian, as the type of statistics of emitted photons is determined by the time integral of the second order correlation function for photons, Eq. (9).[27]

Next, we study dependence of photon noise Fano factor on the photon detection rate. As the photon decay rate decreases, the average photon number in the transmission line increases. At large $\bar{N}$, photons already present in the resonator cause stimulated emission by the DQD[14,28]. For an ideal DQD without energy relaxation, $\gamma_r = 0$, the photon Fano factor grows fast for $\kappa \lesssim \Gamma$, see FIG. 3c. On the other hand, if the energy relaxation in the DQD is significant, the photon Fano factor can exceed unity and the photon field exhibits properties of a thermal state. In this respect, inelastic processes in the DQD enhance photon noise. For strong coupling of the transmission line to the photodetector, $\kappa \gtrsim \gamma_r, g$, and consequently low photon number in the transmission line, the back action of the photon field on electrons is negligible. The adiabatic elimination method[7] can be applied to study photon statistics emitted by a quantum dot, see *e.g.* Ref. 29 and the Supplementary Materials.

Finally, we present the distribution function of the photon counts n over time t_0. For ideal DQD with $\gamma_{\rm r} = \gamma_\phi = 0$, we take $t_0 = 75/\Gamma$ and obtain the distribution $P_n(t_0)$ from Eq. (6), shown in FIG. 4a. The average value of photon counts, $\langle n\rangle = \sum_n nP_n \simeq 27.6$ is consistent with $\langle n\rangle = \bar{N}\kappa t_0$ with $\bar{N} = 0.184$. The variance of photon counts, $\langle n^2\rangle - \langle n\rangle^2 \simeq 11.6$, in turn gives the Fano factor $F_{\rm ph} = 0.42$, which coincides with previous calculation, see Fig. 2d. For comparison, we present the Poisson distribution with the same expectation value $\langle n\rangle$ by narrow black dots in FIG. 4a. Once we consider inelastic processes in the DQD, the distribution is closer to the Poisson distribution, as shown in FIG. 4b, where the vertical bars represent P_n for a system with $\gamma_{\rm r} = 2\Gamma$, $t_0 = 145/\Gamma$, $\langle n\rangle \simeq 27.6$ ($\bar{N} = 0.095$) and $F_{\rm ph} = 0.76$.

Conclusions. We investigated statistics of photons emitted by a biased DQD coupled to a lossless transmission line. We calculated the time correlation function $g^{(2)}_{\rm ph}(\tau)$ and found that the probability to observe two photons simultaneously is smaller than that for longer times, indicating photon antibunching. We also calculated photon counting statistics $P_n(t_0)$ of observing n photons during a fixed time interval t_0. We find that distribution $P_n(t_0)$ shows a sub-Poissonian statistics.

In recent experiments, decoherence rates are comparable to the strength of the electron–photon coupling. For this reason, we investigated the effect on charge and photon statistics of pure dephasing in the DQD and energy relaxation. We found that pure dephasing does not significantly modify the charge transfer or photon emission statistics, but the inelastic relaxation processes result in several drastic changes, see FIG. 2: (*i*) The electric current and its noise acquire strong background as the inelastic processes facilitate the charge transfer throughout the DQD, and the peak in I and the deep in $F_{\rm el}$ at the resonant condition $E_e - E_g = \hbar\omega_0$ are flattened. (*ii*) The photon number $\bar{N}$ at the resonance is suppressed as the effective photon source is reduced due to additional channels for $e \to g$ transition via inelastic events. (*iii*) Photon Fano factor $F_{\rm ph}$ as a function of the level spacing is flatten as well. In the presence of inelastic electron relaxation, the memory time of the DQD is reduced, that increases the photon correlation function $g^{(2)}_{\rm ph}$ at short time scales, see FIG. 3a, and brings photon distribution function to the Poissonian distribution, FIG. 4b.

Acknowledgements. We thank R. McDermott, J. Petta and H. Türeci for fruitful discussions. The work was supported by NSF Grant No. DMR-1105178, ARO and LPS Grant No. W911NF-11-1-0030.

---

[1] R. Glauber, Phys. Rev. **131**, 2766 (1963).

[2] C. Beenakker and H. Schomerus, Phys. Rev. Lett. **86**, 700

(2001); C. Beenakker and H. Schomerus, Phys. Rev. Lett. **93**, 096801 (2004).

[3] A. V. Lebedev, G. B. Lesovik, and G. Blatter, Phys. Rev. B **81**, 155421 (2010).

[4] D. I. Schuster, A. Houck, J. A. Schreier, A. Wallraff, J. M. Gambetta, A. Blais, L. Frunzio, J. Majer, B. Johnson, M. H. Devoret, et al., Nature **445**, 515 (2007); M. Hofheinz, E. M. Weig, M. Ansmann, R. C. Bialczak, E. Lucero, M. Neeley, A. D. O'Connell, H. Wang, J. M. Martinis, and A. N. Cleland, Nature **454**, 310 (2008).

[5] J. Gabelli, L.-H. Reydellet, G. Fève, J.-M. Berroir, B. Plaçais, P. Roche, and D. Glattli, Phys. Rev. Lett. **93**, 056801 (2004).

[6] E. Zakka-Bajjani, J. Ségala, F. Portier, P. Roche, D. Glattli, A. Cavanna, and Y. Jin, Phys. Rev. Lett. **99**, 236803 (2007).

[7] H. J. Carmichael, *Statistical Methods in Quantum Optics 2: Non-Classical Fields* (Springer, 2008).

[8] Y.-F. Chen, D. Hover, S. Sendelbach, L. Maurer, S. Merkel, E. Pritchett, F. Wilhelm, and R. McDermott, Phys. Rev. Lett. **107**, 217401 (2011); A. Poudel, R. McDermott, and M. G. Vavilov, Phys. Rev. B **86**, 174506 (2012), 1201.2990.

[9] T. Frey, P. J. Leek, M. Beck, A. Blais, T. Ihn, K. Ensslin, and A. Wallraff, Phys. Rev. Lett. **108**, 046807 (2012).

[10] K. D. Petersson, L. W. McFaul, M. D. Schroer, M. Jung, J. M. Taylor, A. A. Houck, and J. R. Petta, Nature **490**, 380 (2012), 1205.6767.

[11] H. Toida, T. Nakajima, and S. Komiyama, Phys. Rev. Lett. **110**, 066802 (2013).

[12] W. van der Wiel, S. De Franceschi, J. Elzerman, T. Fujisawa, S. Tarucha, and L. Kouwenhoven, Reviews of Modern Physics **75**, 1 (2002).

[13] L. Childress, A. S. Sørensen, and M. D. Lukin, Phys. Rev. A **69**, 042302 (2004).

[14] P.-Q. Jin, M. Marthaler, J. H. Cole, A. Shnirman, and G. Schön, Phys. Rev. B **84**, 035322 (2011).

[15] J. Jin, M. Marthaler, P.-q. Jin, and D. Golubev (2012), arXiv:1210.5698v1.

[16] C. Xu and M. G. Vavilov, Phys. Rev. B **87**, 035429 (2013).

[17] Y. Blanter and M. Büttiker, Physics Reports **336**, 1 (2000); L. S. Levitov, in *Quantum Noise in Mesoscopic Physics*, edited by Y. Nazarov (Kluwer, 2003).

[18] C. Emary, C. Pöltl, A. Carmele, J. Kabuss, A. Knorr, and T. Brandes, Phys. Rev. B **85**, 165417 (2012), 1201.6323.

[19] D. A. Bagrets and Y. V. Nazarov, Phys. Rev. B **67**, 085316 (2003).

[20] C. Flindt, T. Novotný, and A.-P. Jauho, Europhysics Letters (EPL) **69**, 475 (2005); C. Flindt, T. Novotný, and A.-P. Jauho, Phys. Rev. B **70**, 205334 (2004); T. Brandes, Annalen der Physik **17**, 477 (2008).

[21] D. Marcos, C. Emary, T. Brandes, and R. Aguado, New Journal of Physics **12**, 123009 (2010).

[22] A. A. Clerk, M. H. Devoret, S. M. Girvin, F. Marquardt, and R. J. Schoelkopf, Reviews of Modern Physics **82**, 1155 (2010).

[23] X. Zou and L. Mandel, Phys. Rev. A **41**, 475 (1990).

[24] P. Kelley and W. Kleiner, Phys. Rev. **136**, A316 (1964).

[25] S. Gustavsson, R. Leturcq, B. Simovič, R. Schleser, T. Ihn, P. Studerus, and K. Ensslin, Phys. Rev. Lett. **96**, 076605 (2006).

[26] B. Elattari and S. A. Gurvitz, Physics Letters A **292**, 289 (2002).

[27] While electrons always exhibits antibunching, their transfer statistics can be super-Poissonian[18].

[28] O. Astafiev, K. Inomata, A. O. Niskanen, T. Yamamoto, Y. A. Pashkin, Y. Nakamura, and J. S. Tsai, Nature **449**, 588 (2007).

[29] R. Sánchez, G. Platero, and T. Brandes, Phys. Rev. Lett. **98**, 146805 (2007); R. Sánchez, G. Platero, and T. Brandes, Phys. Rev. B **78**, 125308 (2008).

[30] C. Gardiner and P. Zoller, *Quantum Noise* (Springer, 2008).

Supplementary Materials for "Full Counting Statistics of Photons Emitted by Double Quantum Dot"

S. I. PHOTON EMISSION STATISTICS

S. I. 1. Quantum Jump Approach

In this section we utilize the quantum jump approach[30] to an open quantum system. The Liouvillian for the equation of the motion of the density matrix in Lindblad form can be decomposed as

$$\dot{\rho}(t) = \mathcal{L}\rho(t) = (\mathcal{L}_0 + \mathcal{J})\,\rho(t), \tag{S11}$$

where we have defined the jump superopertor, $\mathcal{J}\rho = \kappa a\rho a^\dagger$, to describe the quantum jump that corresponds to detection of a photon, and $\mathcal{L}_0$ governing the rest of the dynamics of the system. The full density matrix $\rho(t)$ can be resolved in terms of its components $\rho^{(n)}(t)$ representing a process with n photons being counted by the photon detector during a time interval t:

$$\rho(t) = \sum_n \rho^{(n)}(t). \tag{S12}$$

The equation of motions for $\rho^{(n)}(t)$ is

$$\dot{\rho}^{(n)}(t) = \mathcal{L}_0\rho^{(n)}(t) + \mathcal{J}\rho^{(n-1)}(t). \tag{S13}$$

These equations of motion are coupled and therefore are hard to solve. It is more convenient to define the generalized density matrix

$$\tilde{\rho}(t,s) = \sum_n s^n \rho^{(n)}(t), \tag{S14}$$

by introducing the counting variable for photons, s. The equations of motion for the generalized density matrix $\tilde{\rho}(t,s)$ is obtained by multiplying Eq.(S13) by s^n and taking sum over n,

$$\dot{\tilde{\rho}}(t,s) = \mathcal{M}(s)\tilde{\rho}(t,s), \tag{S15}$$

with

$$\mathcal{M}(s) = \mathcal{L}_0 + s\mathcal{J}. \tag{S16}$$

For $s = 1$, Eq. (S15) reduces to the master equation $\dot{\rho}(t) = \mathcal{M}(1)\rho(t)$. The formal solution of Eq. (S15) is

$$\tilde{\rho}(t,s) = e^{\mathcal{M}(s)t}\tilde{\rho}(0,s), \tag{S17}$$

where $\tilde{\rho}(0,s) = \rho_{\rm st}$ is the initial state.

We introduce moment generating function

$$\mathcal{G}(t,s) = \mathrm{Tr}\left\{\tilde{\rho}(t,s)\right\} = \mathrm{Tr}\left\{e^{\mathcal{M}(s)t}\tilde{\rho}(0,s)\right\}. \tag{S18}$$

This function permits one to calculate the full counting statistics, *i.e.* the probability distribution $P_n(t)$ of emission of n photons during time interval t. Indeed, the n resolved density matrix allows us to obtain the full counting statistics of the system by taking trace of $\rho^{(n)}(t)$:

$$P_n(t) = \mathrm{Tr}\{\rho^{(n)}(t)\}. \tag{S19}$$

Then, according to Eqs. (S14) and (S18), we identify

$$\mathcal{G}(t,s) = \sum_n s^n P_n(t). \tag{S20}$$

The probability distribution $P_n(t)$ is given by the inverse Fourier transform in parameter $s = \exp(i\chi)$:

$$P_n(t) = \int_0^{2\pi} e^{-in\chi}\mathcal{G}(t, e^{i\chi})\frac{d\chi}{2\pi}. \tag{S21}$$

The factorial moments of n can be obtained by derivatives of $\mathcal{G}(t,s)$:

$$\left.\frac{\partial^m \mathcal{G}(t,s)}{\partial s^m}\right|_{s=1} = \sum_n P_n(t)\prod_{i=0}^{m-1}(n-i). \tag{S22}$$

We note that Eq. (S17) is understood as a Dyson series, therefore the density matrix can be unravelled into a sum of contributions corresponding to $n = 0, 1, 2, \ldots$ photon detections according to

$$\begin{aligned}\tilde{\rho}(s,t) =& \mathcal{S}(t,0)\rho_{\rm st} + \sum_n \int_0^t dt_n \cdots \int_0^{t_2} dt_1 \\ & \mathcal{S}(t,t_n)s(t_n)\mathcal{J}(t_n)\cdots\mathcal{S}(t_2,t_1)\mathcal{J}(t_1)\mathcal{S}(t_1,0)\rho_{\rm st},\end{aligned} \tag{S23}$$

where $\mathcal{S}(t_{1,}t_2) = \exp\left[\mathcal{L}_0(t_1 - t_2)\right]$.

S. I. 2. Numerical Calculation of the Fano Factor

In principle, the method descibed above can be used not only for analytical calculation of the Fano factor, but for numerical computation as well. However, as shown in Eq. (S22), evaluation of factorial moments involve derivatives of generating function $\mathcal{G}(t,s)$ over s, which is not accurate and neat enough in practice for numerical calculations. In this subsection, we describe a numerical method more suitable for numerical evaluation of Fano factors that we used in the main text.

Our aim is to calculate the photon counts of the system during measurement time t_0 in the steady state,

$$\langle \delta n(t_0)^2\rangle = \frac{1}{2}\int_0^{t_0} dt_1 \int_0^{t_0} dt_2 \left\langle\{\delta\mathcal{J}(t_1), \delta\mathcal{J}(t_2)\}\right\rangle, \tag{S24}$$

where $\delta\mathcal{J}(t) = \mathcal{J}(t) - J(t)$ and $J(t) = \kappa\bar{N}(t) = \mathrm{Tr}\mathcal{J}\rho_{\rm st}$ is the average photon count rate with κ being the measurement rate of photons; $\{A, B\}$ stands for an anticommutator. We can take derivatives of Eq. (S23) over s, and find the correlation function of photon counts during measurement time t_0 in the form $\langle n(t_0)\rangle = \int_0^{t_0} dt J(t)$

and

$$\begin{aligned}\langle n^2(t_0)\rangle &= \int_0^{t_0} dt_1 \int_0^{t_0} dt_2 \left.\frac{\delta^2 \mathrm{Tr}\tilde{\rho}(t_0,s)}{\delta s(t_1)\delta s(t_2)}\right|_{s=1} \\ &+ \int_0^{t_0} dt \left.\frac{\delta \mathrm{Tr}\tilde{\rho}(t_0,s)}{\delta s(t)}\right|_{s=1} \\ &= 2\int_0^{t_0} dt_1 \int_0^{t_1} dt_2 \, \langle \mathcal{J}(t_1)\mathcal{S}(t_1,t_2)\mathcal{J}(t_2)\rangle \\ &+ \langle n(t_0)\rangle.\end{aligned} \tag{S25}$$

Note that we have implied $t_1 \geq t_2$ in the second line and thus the term with $t_1 \leq t_2$ should be added to symmetrize the expression with switching on time labels. Then, one can integrate Eq. (S25) with respect to t_1 and t_2

$$\begin{aligned}\langle \delta n^2\rangle &= \langle n^2(t_0)\rangle - \int_0^{t_0}\int_0^{t_0} dt_1 dt_2 J^2 \\ &= \langle n(t_0)\rangle + 2\int_0^{t_0} d\tau (t_0-\tau)\left[\mathrm{Tr}\left(\mathcal{J}\mathcal{S}(\tau)\mathcal{J}\rho_{\rm st}\right) - J^2\right] \\ &= \langle n(t_0)\rangle + 2J^2\int_0^{t_0} d\tau (t_0-\tau)\left(g^{(2)}(\tau)-1\right),\end{aligned} \tag{S26}$$

and arrives at the celebrated Mandel's photon counting formula.[23] Taking into account that t_0 is large compared to the characteristic memory time of the system, Eq. (S26) reduces to the expression for the photon Fano factor, independent from t_0

$$F = \frac{\langle \delta n^2\rangle}{\langle n(t_0)\rangle} = 1 + 2J\int_0^{\infty} d\tau \mathrm{Tr}\left\{g^{(2)}(\tau)-1\right\}. \tag{S27}$$

Following Ref. 20, we introduce the "Dirac notation" in Liouvillian space for steady state $|\mathrm{st}\rangle\rangle \equiv \rho_{\rm st}$ and a dual vector $\langle\langle e| \equiv \hat{1}$. The inner product defined in Liouvillian space is the trace over the "ket" in state "bra". For example, the inner product of the two former objects is given by $\langle\langle e|\mathrm{st}\rangle\rangle \equiv \mathrm{Tr}\rho_{\rm st} = 1$. It is then useful to define the projector $\mathcal{P} = \mathcal{P}^2 = |\mathrm{st}\rangle\rangle\langle\langle e|$ onto the steady state as well as its complement $\mathcal{Q} = 1-\mathcal{P}$. Note that a useful property of $\mathcal{P}$ is $\mathcal{L}\mathcal{P} = \mathcal{L}|\mathrm{st}\rangle\rangle\langle\langle e| = 0$ and $\mathcal{P}\mathcal{L} = 0$, and therefore $\mathcal{L} = \mathcal{Q}\mathcal{L}\mathcal{Q}$. The propagator $\mathcal{S}(\tau)$ in the second line of Eq. (S26) can be decomposed as $\mathcal{S}(\tau) = \mathcal{P} + \mathcal{Q}\mathcal{S}(\tau)\mathcal{Q}$, and thus $\mathrm{Tr}\left(\mathcal{J}\mathcal{P}\mathcal{J}\rho_{\rm st}\right) = \langle\langle e|\mathcal{J}|\mathrm{st}\rangle\rangle\langle\langle e|\mathcal{J}|\mathrm{st}\rangle\rangle = J^2$. We obtain

$$\begin{aligned}F &= 1 + \frac{2}{J}\int_0^{t_0\to\infty} d\tau \mathcal{J}\mathcal{Q}\mathcal{S}(\tau)\mathcal{Q}\mathcal{J} \\ &= 1 - \frac{2}{J}\mathrm{Tr}\left\{\mathcal{J}\mathcal{Q}\mathcal{L}^{-1}\mathcal{Q}\mathcal{J}\rho_{\rm st}\right\} \\ &= 1 - \frac{2}{J}\langle\langle e|\mathcal{J}\mathcal{R}\mathcal{J}|\mathrm{st}\rangle\rangle,\end{aligned} \tag{S28}$$

where $\mathcal{R} = \mathcal{Q}\mathcal{L}^{-1}\mathcal{Q}$ is the inverse of the Liouvillian projected out of the steady state.

Equation (S28) is the key step in evaluating the photon noise spectrum. We also have to find the inverse of the Loiouvillian, $\mathcal{R}$, and project the result out of the steady state. In practice, inverse of the Liouvillian matrix with large dimension is numerically unstable, but we can evaluate the combination $|\mathcal{W}\rangle\rangle = \mathcal{R}\mathcal{J}|\mathrm{st}\rangle\rangle$ determined by the following equation

$$\begin{aligned}\mathcal{L}|\mathcal{W}\rangle\rangle &= \mathcal{L}\mathcal{R}\mathcal{J}|\mathrm{st}\rangle\rangle = \mathcal{Q}\mathcal{J}|\mathrm{st}\rangle\rangle \\ &= \mathcal{J}|\mathrm{st}\rangle\rangle - |\mathrm{st}\rangle\rangle\langle\langle e|\mathcal{J}|\mathrm{st}\rangle\rangle,\end{aligned} \tag{S29}$$

where the second equality is obtained by the relation $\mathcal{L}\mathcal{R} = \mathcal{L}\mathcal{Q}\mathcal{L}^{-1}\mathcal{Q} = \mathcal{L}(1-\mathcal{P})\mathcal{L}^{-1}\mathcal{Q} = \mathcal{Q}$. To this end, the solution $|\mathcal{W}\rangle\rangle$ in Eq. (S29) is equivalent to the inverse $\mathcal{R}$. In the Liouvillian space the right hand side of Eq.(S29) is a column vector. Therefore, our task is to solve a set of linear equations. At the end of the calculation we fix the solution by projection out of the steady state by condition $\langle\langle e|\mathcal{W}\rangle\rangle = \mathrm{Tr}\left\{\mathcal{R}\mathcal{J}\rho_{\rm st}\right\} = 0$, accomplished by premultiplication of projector $\mathcal{Q}|\mathcal{W}\rangle\rangle$.

S. II. ADIABATIC ELIMINATION OF PHOTON DEGREES OF FREEDOM

In the limit of strong photon relaxation, $\kappa \gg \gamma, g$, the photon degrees of freedom decay so fast that the density matrix can be approximately factorized as

$$\rho(t) \simeq \rho_{\rm DQD}(t)\left(|0\rangle\langle 0|\right), \tag{S30}$$

where $|0\rangle$ is the vacuum state of photon in the transmission line. Thus we can adiabatically eliminate the photon mode, and obtain the equation of motion for the reduced density matrix $\tilde{\rho}_{\rm DQD}(t,s)$ in the interaction picture[7],

$$\dot{\tilde{\rho}}_{\rm DQD}(t,s) = \Gamma_l\mathcal{D}(c_l^\dagger)\tilde{\rho}_{\rm DQD}(t,s) + \Gamma_r\mathcal{D}(c_r)\tilde{\rho}_{\rm DQD}(t,s) + (\gamma_r+\gamma_{\rm ph})\mathcal{D}(\sigma^-)\tilde{\rho}_{\rm DQD}(t,s) + (s-1)\mathcal{J}(\sigma^-)\tilde{\rho}_{\rm DQD}(t,s), \tag{S31}$$

where $\gamma_{\text{ph}} = 4g^2/\kappa$. Note that the photon induced decay rate γ_{ph} is associated with the spontaneous emission in this large κ limit, therefore photon absorptions can be reflected by the jump superoperator $\mathcal{J}(\sigma^-)\tilde{\rho}_{\text{DQD}}(t,s) = \gamma_{\text{ph}}\sigma^-\tilde{\rho}_{\text{DQD}}(t,s)\sigma^+$. In the basis $\rho_{\text{DQD}} = (\rho_0, \rho_g, \rho_{ge}, \rho_{eg}, \rho_e)^T$, the matrix $\mathcal{M}(s)$ in Eq. (S15) is given by:

$$\mathcal{M}(s) = \frac{1}{4}\begin{pmatrix} -4\Gamma_l & -2\Gamma_r\cos\theta + 2\Gamma_r & -\Gamma_r\sin\theta & -\Gamma_r\sin\theta & 2\Gamma_r\cos\theta + 2\Gamma_r \\ 2\Gamma_l\cos\theta + 2\Gamma_l & 2\Gamma_r\cos\theta - 2\Gamma_r & -\Gamma_r\sin\theta & -\Gamma_r\sin\theta & 4\gamma_r + 4s\gamma_{\text{ph}} \\ -2\Gamma_l\sin\theta & -\Gamma_r\sin\theta & -2\Gamma_r - 2\gamma_{\text{t}} & 0 & -\Gamma_r\sin\theta \\ -2\Gamma_l\sin\theta & -\Gamma_r\sin\theta & 0 & -2\Gamma_r - 2\gamma_{\text{t}} & -\Gamma_r\sin\theta \\ -2\Gamma_l\cos\theta + 2\Gamma_l & 0 & -\Gamma_r\sin\theta & -\Gamma_r\sin\theta & -2\Gamma_r\cos\theta - 2\Gamma_r - 4\gamma_{\text{t}} \end{pmatrix}, \tag{S32}$$

where $\gamma_{\text{t}} = \gamma_r + \gamma_{\text{ph}}$.

To calculate the generating function $\mathcal{G}(s,t)$ and its derivatives, we take the Laplace transform of the generalized density matrix, Eq. (S17),

$$\tilde{\rho}(z,s)_{\text{DQD}} = (z - \mathcal{M}(s))^{-1}\tilde{\rho}(0,s)_{\text{DQD}}. \tag{S33}$$

Since the long time behavior of the solution is determined by the residue of the generating function at the pole near $z = 0$, i.e., $\mathcal{G}(t,s) \sim g(s)e^{z_0 t}$ with $g(1) = 1$, we can expand the pole around $s = 1$:

$$z_0 = \sum_{i>0} c_i (s-1)^i, \tag{S34}$$

and obtain, from Eq. (S22), the first two moments, $\langle\langle n^i \rangle\rangle = \langle (n - \langle n \rangle)^i \rangle$:

$$\langle\langle n \rangle\rangle = \left.\frac{\partial g}{\partial s}\right|_{s=1} + c_1 t, \tag{S35}$$

$$\langle\langle n^2 \rangle\rangle = \left.\frac{\partial^2 g}{\partial s^2}\right|_{s=1} - \left(\left.\frac{\partial g}{\partial s}\right|_{s=1}\right)^2 + \left.\frac{\partial g}{\partial s}\right|_{s=1} + (c_1 + 2c_2)\, t, \tag{S36}$$

which give the mean and variance of the probability distribution, respectively. In the asymptotic limit, $t \to \infty$, all the information about the moments is included in the expansion coefficients c_i. For instance, the Fano factor is given by[29]

$$F \equiv \frac{\langle n^2 \rangle - \langle n \rangle^2}{\langle n \rangle} = 1 + \frac{2c_2}{c_1}. \tag{S37}$$

To find the coefficients c_1 and c_2, we consider the equation

$$\det\left(z_0\hat{1} - \mathcal{M}(s)\right) = 0, \tag{S38}$$

with $z_0 = c_1(s-1) + c_2(s-1)^2 + \mathcal{O}\left((s-1)^3\right)$. Then we can expand Eq. (S38) in powers of s and let the coefficients for each power of s be zero. This procedure generates a set of equations with c_i to arbitrary large i. We provide two examples below.

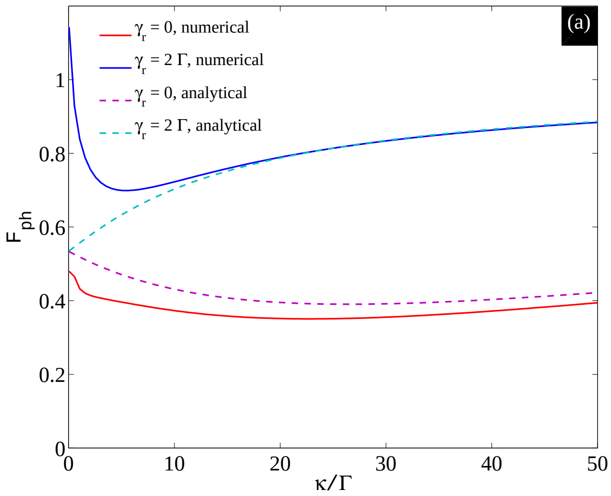

FIG. 5. (Color online) Dependence of photon noise Fano factor on photon decay rate κ at fixed bare coupling constant $g_0 = 5\Gamma$. Solid (dashed) lines represent results for numerical (analytical) calculations with method described in Sec. S.II. Other system parameters are $\Gamma_{l,r} = \Gamma$, $\omega_0 = 800\Gamma$, $\mathcal{T} = 200\Gamma$. Both plots indicate that the analytical results agree with numerical in the limit $\kappa \gtrsim g_0$.

First, considering $\Gamma_l = \Gamma_r = \Gamma$ and $\theta \to \pi$ with fixed coupling constant g, the case in which the two levels in the DQD are weakly overlapping, we obtain

$$c_1 = \frac{\gamma_{\text{ph}}\Gamma}{2\gamma_{\text{tot}} + \Gamma}, \tag{S39}$$

$$c_2 = -\frac{\gamma_{\text{ph}}^2\Gamma(\gamma_{\text{tot}} + 2\Gamma)}{(2\gamma_{\text{tot}} + \Gamma)^3}. \tag{S40}$$

The Fano factor is given by

$$F = 1 - \frac{2\gamma_{\text{ph}}(\gamma_{\text{tot}} + 2\Gamma)}{(2\gamma_{\text{tot}} + \Gamma)^2}, \tag{S41}$$

corresponding to the sub-Poissonian noise. When $\theta = \pi/2$, a case when the DQD is tuned to its charge degen-

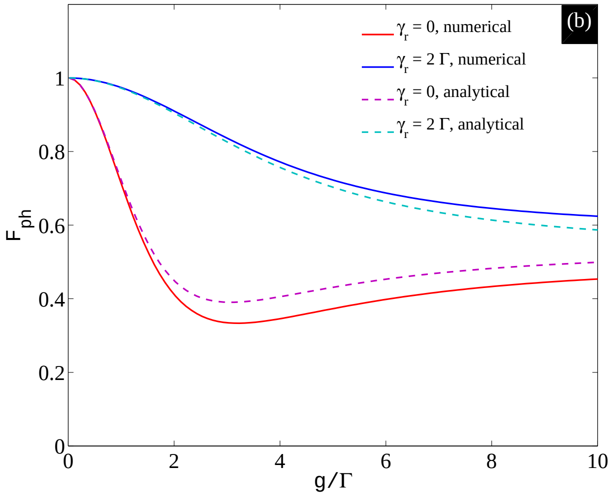

FIG. 6. (Color online) Dependence of photon noise Fano factor on bare coupling constant g_0 at fixed photon decay rate $\kappa = 10\Gamma$. Solid (dashed) lines represent results for numerical (analytical) calculations with method described in Sec. S.II. Other system parameters are $\Gamma_{l,r} = \Gamma$, $\omega_0 = 800\Gamma$, $\mathcal{T} = 200\Gamma$. Both plots indicate that the analytical results agree with numerical in the limit $\kappa \gtrsim g_0$.

eracy, the solutions then read

$$c_1 = \frac{\gamma_{\rm ph}\Gamma(\gamma_{\rm tot} + 2\Gamma)}{6\gamma_{\rm tot}^2 + 11\gamma_{\rm tot}\Gamma + 4\Gamma^2}, \tag{S42}$$

$$c_2 = -\frac{\gamma_{\rm ph}^2\Gamma(\gamma_{\rm tot} + 2\Gamma)\left(4\gamma_{\rm tot}^3 + 14\gamma_{\rm tot}^2\Gamma + 31\gamma_{\rm tot}\Gamma^2 + 20\Gamma^3\right)}{\left(6\gamma_{\rm tot}^2 + 11\gamma_{\rm tot}\Gamma + 4\Gamma^2\right)^3}. \tag{S43}$$

The Fano factor in this case is

$$F = 1 - \frac{2\gamma_{\rm ph}\left(4\gamma_{\rm tot}^3 + 14\gamma_{\rm tot}^2\Gamma + 31\gamma_{\rm tot}\Gamma^2 + 20\Gamma^3\right)}{\left(6\gamma_{\rm tot}^2 + 11\gamma_{\rm tot}\Gamma + 4\Gamma^2\right)^2}, \tag{S44}$$

again, giving the sub-Poissonian noise. In both cases, Fano factors are below 1 if $\gamma_{\rm ph}$ is nonzero, indicating that it is the interaction between photons and electrons that gives rise to the sub-Poissonian statistics.

As mentioned above, this analytical method is valid in the limit when κ is large. We hereby make a comparison between analytical and numerical results, see FIG. 5 and 6. In both plots, we do not consider the effects of dephasing on full counting statistics. The calculation indicate that the analytical method presented above agrees with numerical results in the limit $\kappa \gtrsim g_0$.

S. III. CHARGE TRANSFER STATISTICS

In this section we provide a quick review of the relations for the electric current and current noise through the DQD using the master equation formalism. The current operator is defined as $\hat{I} = e\Gamma_r|R\rangle\langle R| = e\Gamma_r c_r^\dagger c_r$. The dc current is given by the expectation value of $\hat{I}$ with respect to the steady state solution $\rho_{\rm st}$ for the density matrix, see Eq. (4) in the main part of the text:

$$I = e\Gamma_r {\rm Tr}\{|R\rangle\langle R|\,\rho_{\rm st}\}. \tag{S45}$$

The spectral density of the current fluctuations is defined by the relation

$$S(\omega) = \int_{-\infty}^{\infty} \langle\langle \hat{I}(t)\hat{I}(t+\tau)\rangle\rangle e^{i\omega t} dt, \tag{S46a}$$

$$\langle\langle \hat{I}(t)\hat{I}(t+\tau)\rangle\rangle = \left\langle \hat{I}(t)\hat{I}(t+\tau)\right\rangle - I^2. \tag{S46b}$$

The first term in Eq.(S46b) accounts for the concurrence of two electrons at times t and $t+\tau$

$$\langle \hat{I}(t)\hat{I}(t+\tau)\rangle = I^2 g_{\rm el}^{(2)}(t,\tau) + eI\delta(\tau), \tag{S47}$$

where the second order correlation function $g_{\rm el}^{(2)}(\tau)$ is given by

$$g_{\rm el}^{(2)}(\tau) = \frac{{\rm Tr}\left\{c_r^\dagger c_r e^{\mathcal{L}\tau}\left[c_r\rho_{\rm st}c_r^\dagger\right]\right\}}{{\rm Tr}\left\{c_r^\dagger c_r\rho_{\rm st}\right\}^2}, \tag{S48}$$

in terms of the steady state density matrix $\rho_{\rm st}$ and the Liouvillian operator $\mathcal{L}$, see Eq. (4) in the main text. The last term in Eq. (S47) represents counting the same electron at t and $t+\tau$.

Using Eqs. (S46) and (S48), we can write the current noise spectral function in the form:

$$S(\omega) = I^2\int_{-\infty}^{\infty}\left(g_{\rm el}^{(2)}(\tau) - 1\right)e^{i\omega\tau}d\tau + eI. \tag{S49}$$

This result shows that the second order correlation function $g_{\rm el}^{(2)}(\tau)$ is related to the current noise in both frequency and time domains. In particular, the Fano factor $F_{\rm el}$ of the charge current that characterizes the low frequency limit of $S(\omega)$ is[18]

$$F = \frac{S(0)}{eI} = 1 + \frac{2I}{e}\int_0^{\infty}\left(g_{\rm el}^{(2)}(\tau) - 1\right)d\tau. \tag{S50}$$